Catalysis Science & Technology

Accepted Manuscript

ROYAL SOCIETY OF CHEMISTRY

www.rsc.org/catalysis

Journal Name
Catalysis Science & Technology
Dynamic Article Links►

Cite this: DOI: 10.1039/c0xx00000x

www.rsc.org/xxxxxx

ARTICLE TYPE

Facile one-pot fabrication of silica gel-supported chiral phase-transfer catalyst—*N*-(2-cyanobenzyl)-*O*(9)-allyl-cinchonidinium salt

Dandan Feng,[a] Jinghan Xu,[a] Jingwei Wan,[a] Bing Xie *[b] and Xuebing Ma*[a]

Received (in XXX, XXX) Xth XXXXXXXXX 20XX, Accepted Xth XXXXXXXXX 20XX
DOI: 10.1039/b000000x

A novel type of silica gel-supported cinchona alkaloid-based quaternary ammonium salt was prepared by available one-pot synthesis for the first time through the free radical addition of sulfydryl group of 3-mercaptopropyltrimethoxysilane to endocyclic carbon-carbon double bond in *N*-(2-cyanobenzyl)-O(9)-allyl-cinchonidinium bromide, and subsequent hydrolysis of trimethoxysilane. In the α–alkylation of *N*-(diphenylmethylene)glycine *tert*-butyl ester with alkyl halides, it was found that the various substituted benzyl bromides, both with the electron-withdrawing (-CF_3 and -F) and electron-donating (-CH_3) substituents, afforded the corresponding *α*-alkylation products with the moderate to excellent enantioselectivities (76.0–96.9 %ee) in high 80–96% yields. However, allyl bromides gave the poor yields (10–50%) and enantioselectivities (52.0 –67.1 %ee). After the completion of *α*–alkylation reaction, silica gel-supported chiral phase-transfer catalyst could be readily recovered in quantitative yield by filtration, and reused for five consecutive runs without significant loss in catalytic performances.

Introduction

Due to simple experimental procedures, mild reaction conditions, inexpensive and environmentally benign reagents and solvents, phase-transfer catalysis (PTC) has long been recognized as a versatile method to achieve a wide variety of transformations in the field of organic synthesis.[1] Various structurally well-defined non-natural and natural phase-transfer catalysts (PTCs) such as cinchona alkaloid-derived quarternary ammonium salts and *N*-spiro ammonium salts,[2] had been developed, particularly in the last 20 years. Among them, some privileged chiral PTCs have successfully and widely used in the various asymmetric syntheses such as alkylation,[3] conjugate addition,[4] Mannich reaction[5] and Aldol reaction.[6] However, some practical limitations of PTC method are the difficult recovery of homogeneous PTCs and easy formation of stable emulsion. From the point of green chemistry, many endeavors have been devoted to solve these problems. One of them is the immobilization of PTCs on various polymer supports such as Merrifield resin,[7] poly(ethylene glycol)[8] and polystyrene.[9] It is worthwhile to note that these polymer supports have low specific surface areas and obvious shrinkage characteristic in aqueous/organic system, which result in a decline in catalytic performance, compared to the corresponding homogeneous analogues owing to diffusional retardation.

It is well-known that inorganic material is also proved to be an excellent support for the heterogenization of stereoselective organocatalysts due to its excellent thermal and chemical stability, large specific surface area, well-defined tunable pore and adjustable hydrophobic or hydrophilic character.[10] Silica gel is one of these outstanding representatives. [11] However, there has seldom report on the immobilization of homogeneous chiral PTCs into a support with inorganic backbone such as silica gel.[12] Particularly, in the enantioselective *α*-alkylation of *N*-(diph-enylmethylene)glycine *tert*-butyl ester, the strong bases such as concentrated KOH, NaOH or CsOH solution should be required, and could result in a serious corrosion to the inorganic backbone of catalyst support. This may be the reason why there is no report on the inorganic material-supported chiral PTCs used in strong basic medium.

In this paper, we developed a novel type of recoverable silica gel-supported cinchona alkaloid-based quaternary ammonium salt, *N*-(2-cyanobenzyl)-*O*(9)-allyl-cinchonidinium bromide, through available one-pot synthesis for the first time, in which the inorganic backbone of silica was meticulously wrapped by alkyl organic moieties and protected itself from alkali corrosion (**Scheme 1**). In the enantioselective *α*-alkylation of *N*-(diphenylmethylene)glycine *tert*-butyl ester with various *o*, *m*, *p*-substituted benzyl bromides, the moderate to excellent yields (80–96%), enantioselectivities (76.0–96.9%ee) of *α*-alkylation products and satisfactory tolerance of supported PTCs were achieved under optimal conditions.

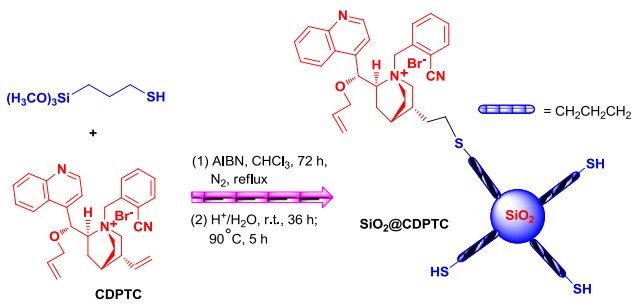

Scheme 1 One-pot synthesis of silica gel-supported cinchona alkaloid-derived PTC catalyst

Experimental

General methods

All chemicals were purchased without further purification. *N*-(2-cyanobenzyl)-*O*(9)-allyl-cinchonidinium bromide (**CDPTC**) was synthesized using cinchonidine (**CD**) as a starting material according to the reference and ascertained by ^{1}H NMR. [13]

The reaction monitoring was accomplished by TLC on silica gel PolyGram SILG/UV254 plates. FT-IR spectroscopy was recorded on a Perkin-Elmer Model GX Spectrometer using KBr pellet method with polystyrene as a standard. Thermogravimetry-differential thermal analysis (TG-DSC) was measured on a SBTQ600 thermal analyzer with a heating rate of 20 ℃ min^{-1} from 40 ℃ to 900 ℃ in air using N_2 as protective gas (100 mL min^{-1}). Elemental analysis of C, H, N, O and S in catalyst was detected from an Vario Micro cube elemental analyzer instrument. The surface morphologies of the samples were determined by a Tecnai G2 F20 transmission electron microscope operated at 200 kV. X-ray powder diffractions were analyzed using a XRD-7000 S/L instrument: Cu-Kα radiation, X-ray tube settings of 40 kV/30 mA and a step size of 2 °min^{-1} in the 10–100 °(2θ) range. N_2 adsorption-desorption analysis was carried out at 77 K on an Autosorb-1 apparatus (Quantachrome), in which the sample was degassed at 120 ℃ for 12 h before measurement. The specific surface area and pore diameter were calculated by the BET method and BJH model, respectively. The enantiomeric excesses (%ee) of α–alkylation products were determined on an Agilent LC-1200 HPLC using Phenomenex Lux 5u Amylose-2 and Daicel Chiralpak OD–H 4.6 mm × 25 cm columns (*n*-hexane/2-propanol = 95/5) under 20 ℃, 254 nm and 0.5 mL min^{-1} conditions.

One-pot preparation of silica gel-supported PTC catalyst

To a sealed round-bottomed flask (100 mL) was charged with *N*-(2-cyanobenzyl)-*O*(9)-allyl-cinchonidinium bromide (265.3 mg, 0.5 mmol), (3-mercaptopropyl)trimethoxysilane (**3-MPTS**, 392.7 mg, 2.0 mmol) and AIBN (16.4 mg, 0.1 mmol), flushed three times with Ar atmosphere. Then $CHCl_3$ (30 mL) was added by a syringe, and the reaction mixture was refluxed for 72 h at 80 ℃ with the monitoring of TLC. During the catalytic reaction, AIBN (16.4 mg, 0.1 mmol) was added once per 24 hours. The reaction mixture was concentrated under reduced pressure, added ethanol-water solution (0.4 mL, *v/v* = 1/1) containing 0.25 mol L^{-1} hydrochloric acid, and then stirred at room temperature for 36 h and at 90 ℃ for 5 h. The formed pale yellow solid was filtered, washed with $CHCl_3$ (2 mL×3), water (2 mL×3) and ethanol (2 mL×3), and dried overnight in *vacuo* to afford silica gel-supported PTC catalyst **SiO_2@CDPTC** (550.0 mg). Anal. Found: C, 48.72; H, 6.18; N, 3.65; O, 1.39; S, 9.87.

General enantioselective α-alkylation reaction

To a mixture of **SiO_2@CDPTC** (0.11 g, 18.8 mol %), *N*-(diphenylmethylene)glycine *tert*-butyl ester (0.15 g, 0.51 mmol), 50 %wt KOH aqueous solution (1.0 mL, 13.4 mmol) and toluene (4.0 mL) was added *o*, *m or p*-substituted benzyl bromide (2.5 mmol) at -40 ℃ and vigorously stirred for 72 h. After the complete consumption of *N*-(diphenylmethylene)glycine *tert*-butyl ester, the reaction mixture was diluted with water (5 mL) and extracted with ether (5 mL×3). The catalyst **SiO_2@CDPTC** was recovered by filtration and reused directly. The combined organic layers were dried over anhydrous Na_2SO_4 and concentrated under reduced pressure to afford the crude product, which was purified by gradient chromatography on alumina gel using petroleum ether/ethyl acetate (*v/v* = 60/1→40/1) as the elu-ents to afford the pure α-alkylation product.

Results and discussion

Chemical composition of the catalyst SiO_2@CD/PTC

As shown in Scheme 1, silica gel-supported *N*-(2-cyanobenzyl)-*O*(9)-allyl-cinchonidinium salt **SiO_2@CDPTC** was prepared conveniently by one-pot method through the free radical addition of sulfydryl in 3-MPTS to endocyclic carbon-carbon double bond in **CDPTC** and subsequent hydrolysis of trimethoxysilane. The free radical addition of endocyclic carbon-carbon double bond was verified by ^{1}H NMR spectra of an analogue of **CDPTC**, which was prepared instead of **3-MPTS** with mercaptan (see ESI†). The covalent attachment of homogeneous **CDPTC** to the inorganic backbone of silica gel was clearly corroborated by FT-IR spectroscopy (Fig.1). The C-H stretching vibrations of =CH, CH, CH_2 and C=C characteristic vibration bands of quinoline ring were confirmed, respectively at 3056, 2925, 2866 cm^{-1} and 1600-1456 cm^{-1} ranges. In particular, the stretching vibrations of the υ_{OH} and υ_{Si-OH} bands with the high relative intensities are very informative. The very strong υ_{OH} stretching vibrations in the 3600–3200 cm^{-1} region were attributed to the hydrogen-bonded silanol groups and adsorbed water on the internal and external surfaces, which elucidated that the catalyst was hydrophilic. The peaks positioned at 1253 and 692 cm^{-1} indicated the stretching vibrations of C-S-C and C-Si bonds, respectively. Furthermore, the characteristic asymmetric stretching (υ_{as}), symmetric stretching (υ_s) and bending modes of Si-O-Si,[14] located at 1029, 766 and 466 cm^{-1} respectively, showed the formation of the inorganic backbone of silica. Therefore, it was concluded that the homogeneous **CDPTC** was successfully anchored into the backbone of silica.

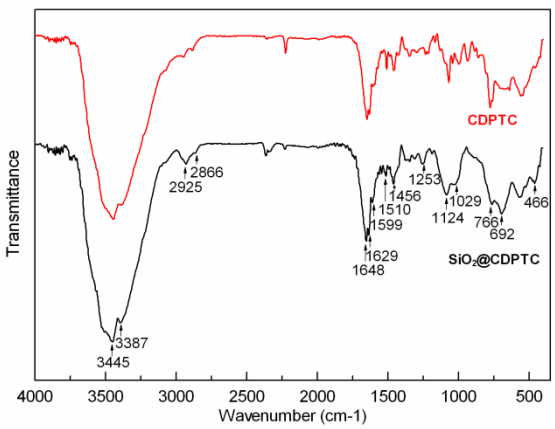

Fig.1 The comparative FT-IR spectroscopy of homogeneous **CDPTC** and supported catalyst **SiO_2@CDPTC**

The loading capacity of homogeneous **CDPTC** in the backbone of silica could be evaluated from the content of nitrogen in **SiO_2@CDPTC** determined by elemental analysis. Based on the content of nitrogen (3.65%), the loading capacity of **CDPTC** was calculated to be 0.87 mmol per gram of **SiO_2@CDPTC**, which

elucidated that 95.7 % of **CDPTC** had been immobilized into the backbone of silica through the one-pot method. Furthermore, according to the contents of nitrogen (3.65 %) and sulfur (9.87 %), the molar ratio of free to **CDPTC**-attached 3-mercaptopropyl organic moieties on the surface of silica was calculated to be 3.54.

Thermogravimetric analysis (TGA) was performed in order to further offer insight, not only into the chemical composition, but also the thermal stability of **CDPTC** attached to **SiO_2@CDPTC**. From the TGA curve (**Fig. 2**), it was found that the thermal decomposition of **SiO_2@CDPTC** occurred in three main steps: the first one with 2.4 % weight loss between 25 ℃ and 100 ℃ corresponded to the surface-bound or intercalated water absorbed in the pores; the second one with the sharp weight loss of 37.4 % between 100 ℃ and 400 ℃, accompanied by an endothermic peak in the DSC curve, was related to the initial decomposition of grafted organic moieties; the third one with the similar sharp weight loss (39.7 %) in the temperature range of 400-730 ℃ was attributed to the further decomposition of organic fragments. Moreover, the total thermal weight loss (77.1 %) in the 100–730 ℃ range was in perfect accord with the total mass (76.8 %) of C, H, N, O, S and Br elements in **SiO_2@CDPTC** by means of elemental analysis and precipitation method using $AgNO_3$ as a precipitant.

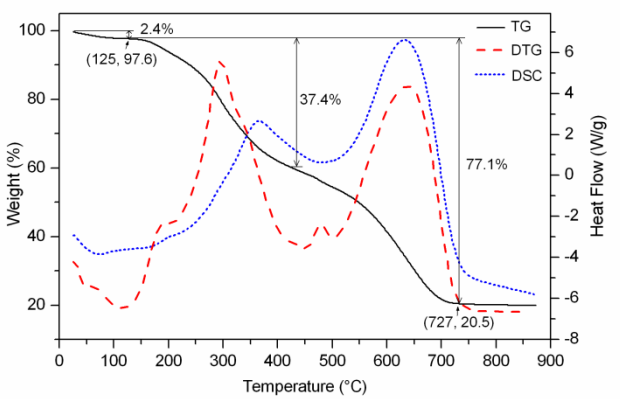

Fig. 2 Thermogravimetric curves of supported catalyst **SiO_2@CDPTC**

Surface morphology

Taking into account the compact relationship between the surface property of supported catalyst and its catalytic performances, it was necessary that **SiO_2@CDPTC** should be well elucidated by SEM and TEM to understand its surface morphology, particle size and pore structure. After being well-dispersed in ethanol (2–3 mg sample in 5 mL of ethanol) under ultrasonic radiation for 10 min, sputtered over copper wire and dried under infrared radiation, the TEM images were observed under an accelerating rate voltage of 200 keV. **Fig. 3** presented the typical scanning electron microscopy (SEM) and transmission electron microscopy (TEM) of **SiO_2@CDPTC**. From the SEM image, **SiO_2@CDPTC** had the micrometer-sized honeycomb-like shape (**Fig. 3a**). The TEM image further showed that **SiO_2@CDPTC** possessed the spherical particles with a uniform diameter of approximate 0.3–0.5 um (**Fig. 3b**), whereas an HRTEM image clearly showed the more delicate surface morphology with the irregular ribbings at the 0.5 –1.5 nm distances (**Fig. 3c**). Furthermore, the electron diffraction pattern (inset of **Fig. 3c**) exhibited an amorphous structure feature of **SiO_2@CDPTC**, which also supported by X-ray diffraction measurements (see ESI†).

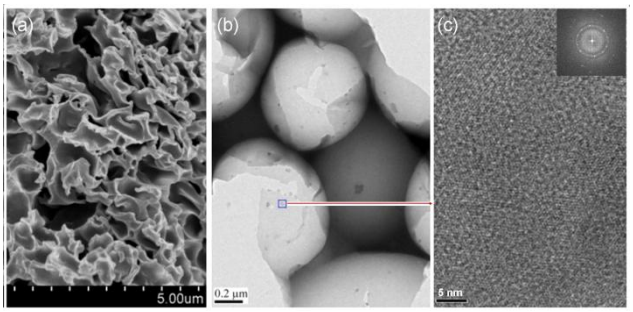

Fig. 3 The surface morphologies of supported catalyst **SiO_2@CDPTC** (a) SEM, (b) TEM and (c) HRTEM images

Porous structure

Nitrogen adsorption–desorption isotherms of **SiO_2@CDPTC** corresponded to the classic definition of Type II isotherm, which matched well with the normal form obtained with a non-porous or macroporous adsorbent (**Fig. 4**). The pore size distribution using the BJH algorithm on the desorption isotherm showed the uneven microporous (<2 nm) and mesoporous (2-30 nm) structures. The BJH curve clearly displayed four peaks with the micropores centered at about 0.9, 1.2, 1.4 and 1.8 nm, and three peaks with the mesopores centered at about 3.6, 4.8 and 7.1 nm (inset of **Fig.4**). Regrettably, from the BET analysis, the low surface area and pore volume of **SiO_2@CDPTC** were calculated to be 0.56 m^2 g^{-1} and 2.72 $\times 10^{-3}$ cc g^{-1}, respectively.

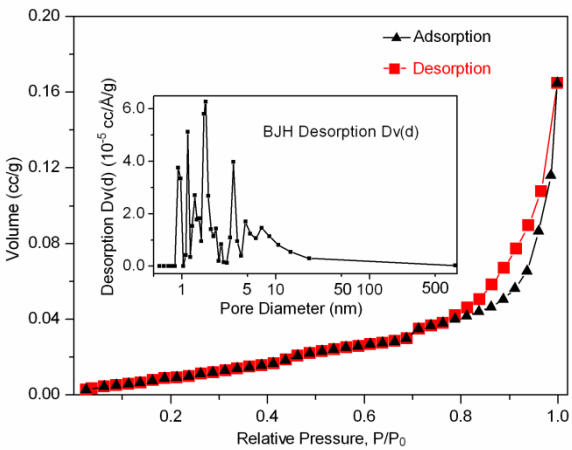

Fig. 4 N_2 adsorption–desorption isotherms of **SiO_2@CDPTC** and pore size distributions from BJH analysis based on desorption isotherm

Catalytic performance

The catalytic efficiency of **SiO_2@CDPTC** was evaluated by the model enantioselective phase-transfer α-alkylation of N-(diphenylmethylene)glycine *tert*-butyl ester, which could produce a large number of natural and non-natural optically active *α*-amino acids.[15]

In order to screen out the optimal reaction conditions, an initial attempt was made by the three-variable screening experiment. As can be seen in **Fig. 5**, the used amount of **SiO_2@CDPTC**, reaction time and temperature had an influence at different degrees on the enantioselectivity, among which the reaction temperature was a key factor that affected the enantioselectivity. The enantioselectivity increased sharply when the reaction temperature decreased

from 10 ℃ to -40 ℃. **SiO_2@CDPTC** (18.8 mol%) gave the 87.1 –90.1 %ee, 93.0–94.1 %ee and 94.1– 96.0 %ee values, respectively at 0 ℃, -20 ℃ and -40 ℃. However, no remarkable difference in enantioselectivity was observed at the different amounts of **SiO_2@CDPTC** in the whole reaction. Furthermore, it was found that the reaction temperature had a significant effect on the yields of the product (**Table 1**). At 0 ℃, all enantioselective *α*–alkylations gave the excellent yields (>98%) at the different amounts of catalyst used. However, with the decrease of reaction temperature, the yields sharply decreased. At -20 and -40 ℃, only *α*-alkylation reaction catalyzed by 18.8 mol% of **SiO_2@CDPTC** produced *α*–alkylation product in an excellent yield (>98%). Therefore, considering two factors of the enantioselectivity and yield, the experimental parameters at -40 ℃ for 72 h with the 18.8 mol% used amount of **SiO_2@CDPTC** were chosen as the optimized reaction conditions applied in the following catalytic experiments.

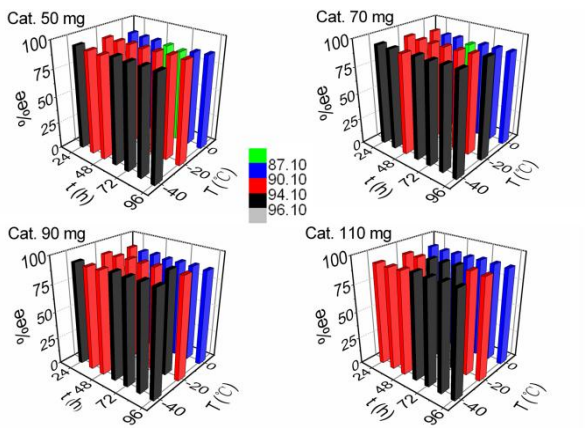

Fig. 5 The enantioselectivities of *α*–alkylation products in the three–variable screening experiments

Encouraged by the remarkable catalytic results of *α*-alkylation of *N*-(diphenylmethylene)glycine *tert*-butyl ester with benzyl bromide, the substrate scope was extended to various *o*, *m*, *p*-substituted benzyl bromides under the optimal catalytic conditions and the results are summarized in **Table 2**. It was found that the various substituted benzyl bromides, both with electron-withdrawing (-CF_3 and -F) and electron-donating (-CH_3) substituents, could produce the corresponding alkylation products with the high enantioselectivities (92.8–96.9 %ee) in good to excellent yields (82–96%) (**entries 1-10**). Moreover, when the benzyl bromides bearing *o*-CF_3, *o*-F and *o*-CH_3 substituents were employed as electrophiles, the slightly lower yields and higher enantioselectivities were observed, which was probably due to the sterically hindered and confined interaction between the *o*-substituents of electrophiles and glycine *tert*-butyl ester controlled by the catalyst **SiO_2@CDPTC** (**entries 3, 6 and 9**).[15] Unfortunately, the enantioselective *α*–alkylation of glycine *tert*-butyl ester with benzyl bromide bearing strong electron-withdrawing NO_2 group (**entries 14-16**) afforded the moderate to good enantioselectivities (76.0–85.6 %) in high yields (90–95%). It was rather disappointing that the allyl bromides gave the poor yields (10–50 %) and unsatisfactory enantioselectivities (52.0 –67.1 %ee) (**entries 11-13**).

Table 1 The yields of enantioselective *α*-alkylation of *N*-(diphenylmethylene)glycine *tert*-butyl ester under different conditions

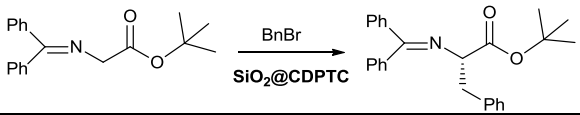

Entry	Used Cat. (mg/mol%)	Temp. (℃)	Isolated yield (%)
1	50/8.5	0	94
2	70/11.9	0	>98
3	90/15.4	0	>98
4	110/18.8	0	>98
5	50/8.5	-20	52
6	70/11.9	-20	65
7	90/15.4	-20	91
8	110/18.8	-20	>98
9	50/8.5	-40	50
10	70/11.9	-40	65
11	90/15.4	-40	81
12	110/18.8	-40	>98

Reaction conditions: 72 h, *N*-(diphenylmethylene)glycine *tert*-butyl ester (0.15 g, 0.51 mmol), BnBr (0.44 g, 2.55 mmol), 50% aq KOH (1.0 mL, 13.4 mmol), toluene (4.0 mL).

Compared with the catalytic efficiency of homogeneous organocatalyst **CDPTC**, **SiO_2@CDPTC** afforded the same excellent enantioselectivities for various benzyl bromides bearing -CF_3, -F and -CH_3 substituents at *o*, *m*, *p*-positions, whereas the poorer enantioselectivities were obtained in heterogeneous catalysis for the allyl bromides (**Table 2**). Moreover, in order to achieve the similar yields as that in homogeneous catalysis, the reaction time in heterogeneous catalysis was prolonged from 7 h to 72 h, which implied the catalytic rates for all the electrophiles dereased dramatically owing to mass transfer of reactants and embedded effect of active sites resulted from the immobilization of **CDPTC** into silical.

The recovery and reuse of catalyst

After the completion of *α*-alkylation reaction, the catalyst **SiO_2@CDPTC** was readily and quantitatively recovered from the reaction mixture by filtration, and directly reused five times without the appreciable drop in the yield and enantioselectivity. Although **SiO_2@CDPTC** was exposed a long time in strong alkali environment during the reaction, it is exciting that the high enantioselectivity (91.6%ee) were retained in the sixth run (**Fig. 6**). However, the yield of *α*–alkylation product significantly decreased to 80% yield in the sixth run. In order to find out the reasons why the catalytic activity of **SiO_2@CDPTC** decreased, several methods such as elemental analysis, SEM, HRTEM, TGA and nitrogen adsorption-desorption isotherm were used to monitor the change of chemical composition, pore structure and surface morphology of the recovered **SiO_2@CDPTC** in the sixth run (**Fig. 6**).

Compared with the fresh catalyst **SiO_2@CDPTC**, the recovered **SiO_2@CDPTC** lost its original micrometer-sized honeycomb-like shape observed from the SEM image, and the TEM image also showed that the fresh regular and spherical particles with a 0.3–0.5 um uniform diameter turned into the irregular particles with about 0.1–0.2 um diameter. The porous structure and surface area of recovered **SiO_2@CDPTC** was further monitored by N_2 adsorption–desorption isotherm. Its surface area and pore volume increased from 0.56 m^2 g^{-1} and 2.72×10^{-3} cc g^{-1} to 4.54 m^2 g^{-1} and 1.47×10^{-2} cc g^{-1} respectively, whereas the average pore diameter

decreased from 9.7 nm to 6.5 nm. From the BJH curve, the pore size distribution showed that the micropores altered little and remained the similar micropores centered at about 0.6, 1.0, 1.2 and 1.9 nm. However, the mesoporous structure had a great change, including the disappeared mesopores at 4.8 nm and 7.1 nm and only one remained mesopore centered at 3.3 nm (inset of **Fig. 7**). Furthermore, the nonuniform microporous structure was obtained after the deep hydrolysis of recovered **SiO_2@CDPTC** in ethanol-water solution containing 0.25 mol L^{-1} hydrochloric acid (see ESI †). Unfortunately, the unsatisfactory enantioselectivity (82.2 %ee) was found. Based on the results described above, it could be concluded that the backbone of amorphous silica collapsed to some extent, and the regularity of porous structure and disappeared mesopores resulted in the decrease in enantioselectivity due to their steric confined effects. In the other hand, the active catalytic site played dominent role in catalytic activity. Superficially, the increased surface area and pore volume of recovered **SiO_2@CDPTC** were better to improve its catalytic activity. However, the weight loss of organic moieties in the temperature range of 150–900 ℃ decreased from 77.1% to 72.7% from the TG curve, which indicated the loss of **CDPTC** in the catalytic process. Therefore, it was conjectured that the loss of organocatalyst **CDPTC** under strong alkali medium was responsible for the decrease in catalytic activity.

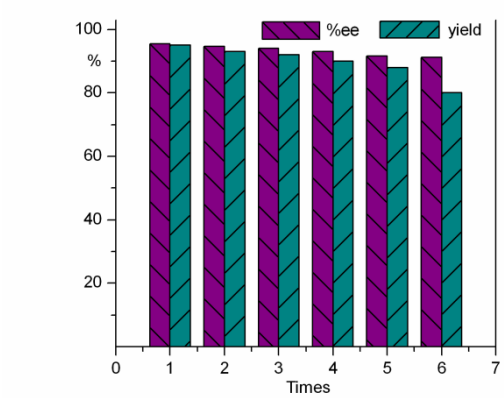

Fig. 6 Reusability of **SiO_2@CDPTC** under optimized reaction conditions

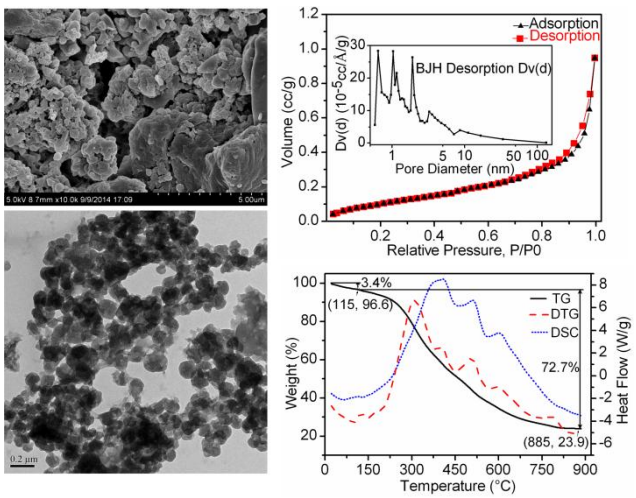

Fig. 7 The SEM, TEM images, TGA and nitrogen adsorption-desorption isotherm of recovered **SiO_2@CDPTC** in the sixth run

Table 2 The enantioselective α-alkylation of *N*-(diphenylmethylene) glycine *tert*-butyl ester using different electrophiles

Entry	Product	Time (h)	Yield (%)[a]	%ee[b]
1	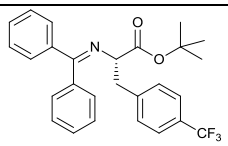	72 10	80 95	93.0 (S) 95.3 (S)[d]
2	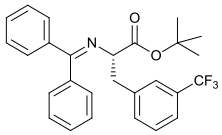	72 10	82 94	93.7 (S)[c] 96.2 (S)[d]
3	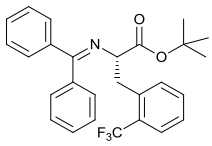	72 10	85 95	95.2 (S) 97.0 (S)[d]
4	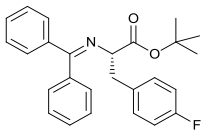	72 10	95 95	93.1 (S) 95.6 (S)[d]
5	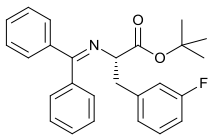	72 10	91 95	93.3 (S) 95.9 (S)[d]
6	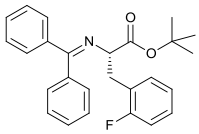	72 10	95 96	95.0 (S) 96.7 (S)[d]
7	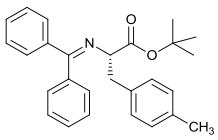	72 7	90 96	95.7 (S) 96.3 (S)[d]
8	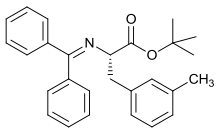	72 7	85 95	92.8 (S) 96.3 (S)[d]
9	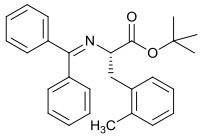	72 7	82 96	96.9 (S) 97.0 (S)[d]
10	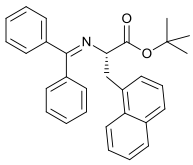	72 10	96 96	93.6 (S) 95.2 (S)[d]

11	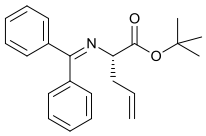	72 7	10 93	57.8 (S) 96 (S) [e]
12	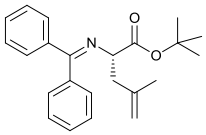	72 7	16 95	52.0 (S) 97 (S) [e]
13	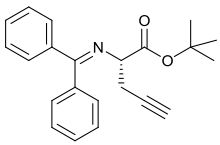	72 7	50 92	67.1 (S) 98 (S) [e]
14	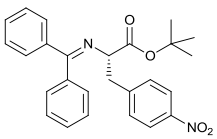	48 7	90 93	76.0 (S) 98 (S) [e]
15	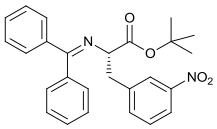	48 5	95 95	85.6 (S) 94.9 (S) [d]
16	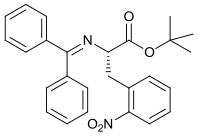	48 5	95 95	82.1 (S) 92.7 (S) [d]

Reaction conditions: 20 mol% **SiO_2@CDPTC**, -40 ℃, substituted benzyl bromide (2.5 mmol), *N*-(diphenylmethylene)glycine *tert*-butyl ester (0.15 g, 0.51 mmol), 50% aq KOH (1.0 mL, 13.4 mmol), 4.0 mL toluene. [a] Isolated yield. [b] Determined by chiral HPLC with Phenomenex Lux 5u Amylose-2 chiral column. [c] Daicel Chiralpak OD-Hcolumn. [d] Homogeneous catalysis by **CDPTC**. [e] The cited %ee from ref. 13 catalyzed by **CDPTC** at -20 ℃.

Conclusions

A novel type of amorphous silica gel-supported PTC catalyst, *N*-(2-cyanobenzyl)-*O*(9)-allyl-cinchonidinium bromide, was prepared through a simple and available one-pot synthesis. The effective immobilization of *N*-(2-cyanobenzyl)-*O*(9)-allyl-cinchonidinium bromide was confirmed by means of elemental analysis and TGA. The catalyst was the first example of inorganic backbone-supported PTC catalyst applied in the enantioselective α-alkylation of *N*-(diphenylmethylene)glycine *tert*-butyl ester with a variety of substituted benzyl bromides, leading to the corresponding α-alkylation products in good to high yields as well as excellent enantioselectivities. The catalyst could tolerate the serious corrosion of strong base, and easily recovered by filtration and reused sixth times with the slight decrease in enantioselectivity.

Acknowledgements

We are grateful to the National Science Foundation of China (21362005, 21071116) and Chongqing Scientific Foundation (CSTC, 2010BB4126).

Notes and references

[a] *Key Laboratory of Applied Chemistry of Chongqing Municipality, School of Chemistry and Chemical Engineering, Southwest University, Chongqing, 400715, P. R. China. Fax: (+86)23-68253237; Tel: (+86)23-68253237; E-mail: zcj123@swu.edu.cn*

[b] *School of Chemistry and Environmental Science, Guizhou Minzhu University, Guiyang, 550025, P. R. China. Fax: (+86)851-3610278; Tel: (+86)851-3610278; E-mail:bing_xie1963@hotmail.com*

† Electronic Supplementary Information (ESI) available: ^{1}H and ^{13}C NMR spectra of α-alkylation products; HPLC spectra of racemic and enantioselective alkylation products; XRD diffraction of **SiO_2@CDPTC**. See DOI: 10.1039/b000000x/

1 (a) T. Ooi and K. Maruoka, *Angew. Chem. Int. Ed*., 2007, **46**, 4222; (b) S. Shirakawa and K. Maruoka, *Angew. Chem. Int. Ed*., 2013, **52**, 4312.

2 (a) T. Marcelli and H. Hiemstra, *Synthesis*, 2010, 1229; (b) K. Kacprzak and J. Gawroński, *Synthesis*, 2001, 961; (c) T. Kano, Q. Lan, X. Wang and K. Maruoka, *Adv. Synth. Catal*., 2007, **349**, 556; (d) S. Shirakawa, M. Ueda, Y. Tanaka, T. Hashimoto and K. Maruoka, *Chem. Asian J*., 2007, **2**, 1276; (e) T. Ooi, Y. Uematsu, M. Kameda and K. Maruoka, *Angew. Chem. Int. Ed.*, 2002, **41**, 1551; (f) T. Ooi, Y. Uematsu, M. Kameda and K. Maruoka, *Tetrahedron*, 2006, **62**, 11425; (g) M. Waser, K. Gratzer, R. Herchl and N. Müller, *Org. Biomol. Chem*., 2012, **10**, 251; (h) M. Kitamura, Y. Arimura, S. Shirakawa and K. Maruoka, *Tetrahedron Lett*., 2008, **49**, 2026; (i) M. Kitamura, S. Shirakawa, Y. Arimura, X. Wang and K. Maruoka, *Chem. Asian J*., 2008, **3**, 1702; (j) Y. Wang and K. Maruoka, *Org. Process Res. Dev*., 2007, **11**, 628; (k) Y. Wang, M. Ueda, X. Wang, Z. Han and K. Maruoka, *Tetrahedron*, 2007, **63**, 6042; (l) B. Lygo, B. Allbutt, D. J. Beaumont, U. Butt and J. A. R. Gilks, *Synlett*., 2009, 675; (m) B. Lygo, U. Butt and M. Cormack, *Org. Biomol. Chem.*, 2012, **10**, 4968.

3 (a) J. Lv, L. Zhang, L. Liu and Y. Wang, *Chem. Lett.*, 2007, **36**, 1354; (b) X. Wang, J. Lv, L. Liu, Y. Wang and Y. Wu, *J. Mol. Catal. A*, 2007, **276**, 102; (c) W. He, Q. Wang, Q. Wang, B. Zhang, X. Sun and S. Zhang, *Synlett*., 2009, 1311; (d) S. E. Denmark and R. C. Weintraub, *Heterocycles*, 2011, **82**, 1527; (e) J. H. Lee, M. S. Yoo, J. H. Jung, S. s. Jew, H. g. Park and B. S.Jeong, *Tetrahedron*, 2007, **63**, 7906; (f) T. Kano,Q. Lan, X.Wang and K. Maruoka, *Adv. Synth. Catal*., 2007,**349**, 556; (g) S. Shirakawa, M. Ueda, Y. Tanaka, T. Hashimoto and K. Maruoka,*Chem. Asian J*., 2007, **2**, 1276; (h) Y.-G. Wang and K. Maruoka, *Org. Process Res. Dev*., 2007, **11**,628; (i) B. Lygo, U. Butt and M. Cormack, *Org.Biomol. Chem.*, 2012, **10**, 4968.

4 (a) T. Ma, X. Fu, C. W. Kee, L. Zong, Y. Pan, K. W. Huang and C. H.Tan, *J. Am. Chem. Soc*., 2011, **133**, 2828; (b) M. Q. Hua, L. Wang, H. F. Cui, J. Nie, X. L. Zhang and J. A. Ma, *Chem. Commun*., 2011, **47**, 1631; (c) S. Shirakawa, Y. Liu, A. Usui and K. Maruoka, *ChemCatChem*, 2012, **4**, 980; (d) H. Kawai, Y. Sugita, E. Tokunaga, H. Sato, M. Shiro and N. Shibata, *Chem. Commun*., 2012, **48**, 3632; (e) J. Nie, M. Q. Hua, H. Y. Xiong, Y. Zheng and J. A. Ma, *J. Org. Chem*., 2012, **77**, 4209; (f) Y. J. Lee, Y. Park, M. h. Kim, S. s. Jew and H. g. Park, *J. Org.Chem*., 2011, **76**, 740; (g) T. Shibuguchi, H. Mihara, A. Kuramochi, S. Sakuraba, T. Ohshima and M. Shibasaki, *Angew.Chem. Int. Ed*., 2006, **45**, 4635; (h) Y. G. Wang, T. Kumano, T. Kano and K. Maruoka, *Org. Lett*., 2009, **11**, 2027; (i) T. Kano, T. Kumano and K. Maruoka, *Org. Lett*., 2009, **11**, 2023.

5 (a) F. Fini, V. Sgarzani, D. Pettersen, R. P. Herrera, L. Bernardi and A. Ricci, *Angew. Chem. Int. Ed*., 2005, **44**, 7975; (b) E. Gomez-Bengoa, A. Linden, R. López, I. Múgica-Mendiola, M. Oiarbide and C. Palomo, *J. Am. Chem. Soc*., 2008, **130**, 7955; (c) Y. Wei, W. He, Y. Liu, P. Liu and S. Zhang, *Org. Lett.*, 2012, **14**, 704; (d) C. Cassani, L. Bernardi, F. Fini and A. Ricci, *Angew.Chem. Int. Ed.*, 2009, **48**, 5694; (e) K. Ohmatsu, A. Goto and T. Ooi, *Chem. Commun*., 2012, **48**, 7913; (f) Y. J. Chen, K. Seki, Y. Yamashita and S. Kobayashi, *J. Am. Chem. Soc*., 2010, **132**, 3244; (g) C. B. Jacobsen, M. Nielsen, D. Worgull, T. Zweifel, E. Fisker and K. A. Jorgensen, *J. Am. Chem. Soc*., 2011, **133**, 7398.

6 (a) B. Ma, J. L. Parkinson and S. L. Castle, *Tetrahedron Lett.*, 2007, **48**, 2083; (b) T. Ooi, M. Taniguchi, M. Kameda and K. Maruoka, *Angew. Chem. Int. Ed.*, 2002, **41**, 4542; (c) T. Ooi, M. Kameda, M. Taniguchi and K. Maruoka, *J. Am. Chem. Soc*., 2004, **126**, 9685; (d)

S. Shirakawa, K. Ota, S. J. Terao and K. Maruoka, *Org. Biomol. Chem.*, 2012, **10**, 5753.

7 (a) R. Chinchilla, P. Mazón and C. Nájera, *Adv. Synth. Catal*., 2004, **346**, 1186; (b) M. J. Kim, S. s. Jew, H. g. Park and B. S. Jeong, *Eur. J. Org. Chem.*, 2007, 2490; (c) Q. Shi, Y. J. Lee, M. J. Kim, M. K. Park, K. Lee, H. Song, M. Cheng, B. S. Jeong, H. g. Park and S. s. Jew, *Tetrahedron Lett.*, 2008, **49**, 1380.

8 (a) J. Lv, X. Wang, J. Liu, L. Zhang and Y. Wang, *Tetrahedron: Asymmetry*, 2006, **17**, 330; (b) A. R. Kiasat, R. Badri, B. Zargar and S. Sayyahi, *J. Org. Chem*., 2008, **73**, 8382.

9 (a) R. Chinchilla, P. Mazón and C. Nájera, *Molecules*, 2004, **9**, 349; (b) Y. Arakawa, N. Haraguchi and S. Itsuno, *Angew. Chem. Int. Ed*., 2008, **47**, 8232; (c) Y. Qin, G. Yang, L. Yang, J. Li and Y. Cui, *Catal. Lett*., 2011, **141**, 481.

10 (a) V. Polshettiwar, R. Luque, A. Fihri, H. Zhu, M. Bouhrara and J.-M. Basset, *Chem. Rev*., 2011, **111**, 3036; (b) A. F. Trindade, P. M. P. Gois and C. A. M. Afonso, *Chem. Rev*., 2009, **109**, 418; (c) J. Wan, L. ding, T. Wu, X. Ma and Q. Tang, *RSC Adv.*, 2014, **4**, 38323; (d) W. Wang, X. Ma, J. Wan, J. Cao and Qian Tang, *Dalton Trans*., 2012, **41**, 5715. (e) S. L. Jain, A. Modak and A. Bhaumik, *Green Chem.*, 2011, **13**, 586; (f) P. García-García, A. Zagdoun, C. Copéret, A. Lesage, U. Díaza and A. Corma, *Chem. Sci*., 2013, **4**, 2006; (g) R. Wang, J. Wan, X. Ma, X. Xu and L. Liu, *Dalton Trans*., 2013, **42**, 6513; (h) T. Chen, X. Ma, X. Wang, Q. Wang, J. Zhou and Q. Tang, *Dalton Trans*., 2011, **40**, 3325.

11 (a) D. Susanti , L. L. R. Ng and P. W. H. Chan, *Adv. Synth. Catal*., 2014, **356**, 353; (b) C. Wang, B. Luo, X. M. Li, X. Q. Cao, Y. Pan and H. W. Gu, *RSC Adv*., 2014, **4**, 15036; (c) E. Montroni, M. Lombardo, A. Quintavalla, C. Trombini, M. Gruttadauria and F. Giacalone, *ChemCatChem*, 2012, **4**, 1000; (d) H. Gruber-Woelfler, G. J. Lichtenegger, C. Neubauer, E. Polo and J. G. Khinast, *Dalton Trans*., 2012, **41**, 12711; (e) P. N. Liu, F. Xia, Q. W. Wang, Y. J. Ren and J. Q. Chen, *Green Chem*., 2010, **12**, 1049; (f) P. Nandi, J. L. Dye, P. Bentley and J. E. Jackson, *Org. Lett*., 2009, **11**, 1689.

12 L. Li, J. Shi, J. Yan, H. Chen and X. Zhao, *J. Mol. Catal. A: Chem.*, 2004, **209**, 227.

13 M. S. Yoo, B. S. Jeong, J. H. Lee, H. g. Park and S. s. Jew, *Org. Lett*., 2005, **7**, 1129.

14 (a) A. Khalafi-Nezhad and F. Panahi, *Green Chem.*, 2011, **13**, 2408; (b) A. Khalafi-Nezhad, E. S. Shahidzadeh, S. Sarikhani and F. Panahi, *J. Mol. Catal. A: Chem.*, 2013, **379**, 1.

15 (a) T. Kano, T. Kumano, R. Sakamoto and K. Maruoka, *Org. Biomol. Chem.*, 2013, **11**, 271; (b) W. Peng, J. Wan,B. Xie and X. Ma, *Org. Biomol. Chem*., 2014, **12**, 8336; (c) M. Waser, K. Gratzer, R. Herchl and N. Müller, *Org. Biomol. Chem*., 2012, **10**, 251; (d) Y. Du, D. Feng, J. Wan, X. Ma, *Appl. Catal. A: General*, 2014, 479, 49; (e) H. Zhang, D. Feng, H. Sheng, X. Ma, J. Wan and Q. Tang, *RSC Adv.*, 2014, **4**, 6417.